

# IMPROVED EVIDENCE FOR A $3 \times 10^6 M_\odot$ BLACK HOLE IN M32: CANADA-FRANCE-HAWAII TELESCOPE SPECTROSCOPY WITH FWHM = $0''.47$ RESOLUTION

RALF BENDER

Universitäts-Sternwarte, Scheinerstraße 1, München 81679, Germany; bender@usm.uni-muenchen.de

JOHN KORMENDY<sup>1</sup>

Institute for Astronomy, University of Hawaii, 2680 Woodlawn Drive, Honolulu, HI 96822; kormendy@ifa.hawaii.edu

AND

WALTER DEHNEN

University of Oxford, Theoretical Physics, 1 Keble Road, Oxford OX1 3NP, England; dehnen@thphys.ox.ac.uk

Received 1996 February 5; accepted 1996 April 3

## ABSTRACT

We present improved spectroscopy of M32 with the Canada-France-Hawaii Telescope and Subarcsecond Imaging Spectrograph. Tip-tilt guiding provides a resolution of FWHM =  $0''.47$  or  $\sigma_* = 0''.20$  ( $\sigma_*$  = Gaussian dispersion radius of the point-spread function). The observed central velocity dispersion,  $\sigma \simeq 92 \pm 5 \text{ km s}^{-1}$ , and the maximum rotation velocity,  $V_{\text{max}} = 55 \pm 3 \text{ km s}^{-1}$ , are larger than at lower resolution. In addition, the measured line-of-sight velocity distributions indicate the possible presence of broad wings at radii  $r \lesssim 0''.2$ , with significant numbers of stars at  $\Delta V \simeq 200 \text{ km s}^{-1}$  from the mean velocity. Two-integral dynamical models fit these data provided that M32 contains a central dark object, probably a black hole, of mass  $M_\bullet \simeq (3.0 \pm 0.5) \times 10^6 M_\odot$ . This confirms detections based on lower resolution spectra by Tonry, Dressler, Richstone, van der Marel, Dehnen, and collaborators. The available spatial resolution has now improved by a factor of 3 since Tonry's discovery observations; each improvement in resolution has strengthened the case for a black hole in M32.

*Subject headings:* black hole physics — galaxies: individual (M32) — galaxies: kinematics and dynamics — galaxies: nuclei

## 1. INTRODUCTION

M32 was the first galaxy with convincing evidence (Tonry 1984, 1987) for a central massive dark object (MDO), probably a black hole (BH)—an extinct remnant of a once active nucleus. It is now the most thoroughly studied BH candidate (see Kormendy & Richstone 1995, hereafter KR95, for a review). Tonry measured its rotation curve,  $V(r)$ , and velocity dispersion profile,  $\sigma(r)$ , with seeing  $\sigma_* \sim 0''.5$ – $0''.85$ . Isotropic dynamical models fitted to these data implied that the mass-to-light ratio  $M/L$  increases toward the center. Tonry concluded that M32 contains a BH of mass  $M_\bullet \sim (3$ – $10) \times 10^6 M_\odot$ . Since this work, other groups have improved the spatial resolution, most recently to  $\sigma_* = 0''.32$  (van der Marel et al. 1994a, b). This Letter improves it to  $\sigma_* = 0''.20$ . Each improvement in resolution, together with some important progress in analysis (see below), has strengthened the case that an MDO is present and that it is in fact a BH.

A brief review is in order. Dressler & Richstone (1988) obtained spectra at resolution  $\sigma_* = 0''.45$ . Using maximum entropy dynamical models (Richstone & Tremaine 1988), they showed that velocity anisotropy provides no escape from the conclusion that M32 contains an MDO. Van der Marel et al. (1994a, b) obtained additional spectra at  $\sigma_* = 0''.32$  and measured the Gauss-Hermite coefficients  $h_n$  of the line-of-sight velocity distributions (LOSVDs). They, Qian et al. (1995), and Dehnen (1995) constructed models with two-integral distribution functions  $f(E, L_z)$ , where  $E$  is the total

energy and  $L_z$  is the axial component of angular momentum. Good fits to  $\sigma(r)$  and  $V(r)$  are only obtained when an MDO of mass  $M_\bullet = (1.8 \pm 0.3) \times 10^6 M_\odot$  is included. These results are in good agreement with the conclusions of Tonry, Dressler, and Richstone. They improve on earlier analyses by making flattened models, by fitting the non-Gaussian LOSVDs, and by fitting kinematic observations at a variety of slit positions. They also have an important shortcoming compared to the maximum entropy models:  $f$  is restricted to be a function of two integrals. Such models may fail to fit the data without an MDO, but we cannot prove that more general models also fail. In contrast, the maximum entropy models can be forced to have the smallest possible  $M/L$  as  $r \rightarrow 0$ . When this fails, an MDO is required. Thus the distribution function and maximum entropy models are complementary.

As in all BH candidates, suggestions that the MDO is a BH are based on astrophysical arguments that are less direct than the dynamical arguments for a large  $M/L$  ratio. In this respect, M32 is a better than average case. *Hubble Space Telescope* photometry by Lauer et al. (1992) shows that any core has a radius of less than  $0.37 \text{ pc}$  and that the stellar density reaches  $\rho_* > 3 \times 10^7 M_\odot \text{ pc}^{-3}$ . The relaxation and stellar collision times are short. At  $\sigma \sim 10^2 \text{ km s}^{-1}$ , stellar collisions tend to result in coalescence; they are more likely to lead to a runaway merger instability than in a low- $\sigma$  globular cluster. Kormendy & McClure (1993) make the same point. Lauer and collaborators argue that a BH is favored over other types of MDOs.

What we need next is better spatial resolution to see whether the BH case becomes stronger or weaker. This Letter presents a factor of 1.6 improvement in spatial resolution.

<sup>1</sup> Visiting Astronomer, Canada-France-Hawaii Telescope, operated by the National Research Council of Canada, the Centre National de la Recherche Scientifique of France, and the University of Hawaii.

## 2. CANADA-FRANCE-HAWAII TELESCOPE SIS SPECTROSCOPY

The Subarcsecond Imaging Spectrograph (SIS) was designed for high-resolution work. Its optics are much better than the seeing. The scale is  $0''.0864 \text{ pixel}^{-1}$ ; the slit was  $0''.353 \pm 0''.002$  wide by 2.5 long. Tip-tilt guiding is incorporated; by offsetting the guide probe, we were able to center the object on the slit to better than 1 pixel accuracy. As a result, the resolution is limited only by seeing and by telescope aberrations.

The spectra were taken near the Ca II infrared triplet, at 8025–9030 Å. The reciprocal dispersion was  $0.98 \text{ Å pixel}^{-1} = 34.6 \text{ km s}^{-1} \text{ pixel}^{-1}$ . The spectral resolution was measured to be  $\sigma_{\text{inst}} = 80 \text{ km s}^{-1}$ . Two integrations were obtained, as summarized in Table 1.

It is critical to measure the object centering and the seeing as accurately as possible. We therefore took the following exposure sequences: (1) a direct image to measure the object position and seeing, (2) a direct image with the slit in place to measure the slit position, (3) the spectrum, (4) another direct image with the slit in place, and (5) a final image with no slit to remeasure the seeing and object position (only exposures 1–4 were obtained for spectrum 70f288 because of morning twilight). The centering accuracy and the relevance to the spectrum of the seeing in the direct images can then be checked by comparing brightness cuts along the major axis in images 1–5. The results are shown in Figure 1. For the highest resolution spectrum, 70f288, the galaxy was centered by maximizing the signal through the slit. In this spectrum, the brightness profile of M32 is as centrally peaked as in the direct images. Therefore the centering is good, and the seeing is the same in the images and in the spectrum. We obtain  $\sigma_* = 0''.20 \pm 0''.01$ , or FWHM =  $0''.47 \pm 0''.03$ . This is the highest resolution spectrum that we have obtained in 10 years of BH spectroscopy at the Canada-France-Hawaii Telescope.

Spectrum 70f279 is not as good: the exposure was longer (Table 1), and the galaxy drifted by 1.3 pixels during the integration. We adopt  $\sigma_* = 0''.22 \pm 0''.02$  (FWHM =  $0''.52$ ).

For convolutions, we need the complete point-spread function (PSF) and not just  $\sigma_*$ . We therefore fitted a modified Moffat (1969) function,

$$I(r) = \frac{I_0}{[1 + (r/a_*)^{m_*}]^{n_*}},$$

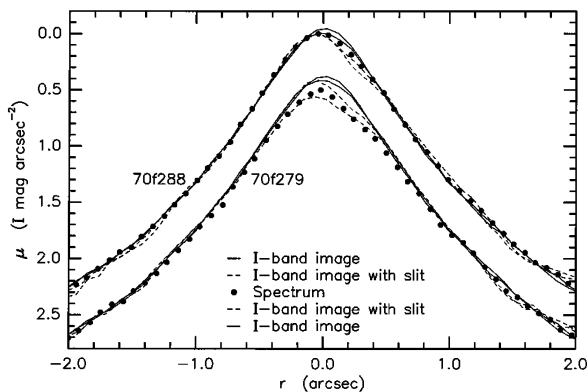


FIG. 1.—Surface brightness cuts through M32 spectra 70f279 and 70f288 and through the bracketing direct images with and without the slit in place. The magnitude zero point is arbitrary.

to the composite star profile relevant to spectrum 70f288. Here  $I(r)$  is the PSF in intensity units and  $a_* = 0''.323$ ,  $m_* = 2.40$ , and  $n_* = 1.69$  are fitting parameters. The fit was excellent out to  $r = 6''.3$ , i.e.,  $12 \text{ mag arcsec}^{-2}$  below the central surface brightness of the PSF.

Velocities  $V$  and velocity dispersions  $\sigma$  were calculated with the Fourier quotient (FQ) program that was used in previous BH spectroscopy (Kormendy 1988a, b; Kormendy & Richstone 1992). We also measured  $V$ ,  $\sigma$ , the higher order Gauss-Hermite coefficients  $h_3$  and  $h_4$ , and nonparametric LOSVDs using Bender's (1990) Fourier correlation quotient (FCQ) program. The two programs agree well: when LOSVD wings are taken into account, the velocity differences between the programs are  $\lesssim 2 \text{ km s}^{-1}$ . Further analysis is based on the FCQ results (Table 1).

Error estimates are based on Monte Carlo simulations to find out how well we recover known values of  $V$ ,  $\sigma$ ,  $h_3$ , and  $h_4$ . In each simulation, one of the above parameters was varied, and the distribution of all output parameters was determined for 30 realizations of spectra with the noise characteristics of the observations. Because our spectral resolution is similar to the velocity dispersion in M32, the derived parameters are affected not only by random noise but also by systematic bias

TABLE 1  
FCQ KINEMATIC RESULTS

$r$	$V$	$\epsilon(V)$	$\sigma$	$\epsilon(\sigma)$	$h_3$	$h_4$	$\epsilon(h_3, h_4)$
M32 Major Axis, Spectrum 70f288 <sup>a</sup>							
−3.88.....	−53	5	51	6	0.043	−0.056	0.090
−2.08.....	−59	5	61	6	0.108	−0.009	0.066
−1.02.....	−52	4	56	4	0.016	−0.015	0.057
−0.62.....	−57	3	62	4	0.099	0.009	0.045
−0.41.....	−43	5	76	5	0.028	−0.049	0.055
−0.23.....	−27	5	92	5	0.047	−0.012	0.042
−0.11.....	−15	6	92	8	0.043	0.025	0.059
−0.02.....	3	6	91	8	−0.016	0.090	0.054
0.07.....	18	6	93	8	−0.017	0.114	0.052
0.15.....	18	5	88	6	−0.022	−0.009	0.051
0.24.....	28	6	88	7	−0.039	0.031	0.054
0.33.....	39	7	82	10	−0.118	0.095	0.071
0.45.....	45	7	78	9	0.001	0.047	0.075
0.63.....	55	5	68	6	−0.094	0.022	0.060
0.84.....	55	6	61	8	−0.067	0.016	0.086
1.44.....	56	4	67	4	−0.052	−0.009	0.045
3.49.....	54	1	65	1	−0.128	0.000	0.014
M32 Major Axis, Spectrum 70f279 <sup>b</sup>							
−4.02.....	−47	6	62	7	0.061	−0.017	0.087
−2.23.....	−61	3	57	4	0.118	−0.006	0.044
−1.17.....	−53	4	62	4	−0.003	−0.017	0.048
−0.76.....	−51	5	66	6	−0.045	0.008	0.063
−0.55.....	−47	3	70	5	0.043	0.067	0.041
−0.37.....	−43	3	70	4	0.089	0.033	0.038
−0.25.....	−38	5	90	6	0.096	−0.049	0.048
−0.16.....	−16	5	91	8	−0.031	0.095	0.050
−0.07.....	−6	6	85	8	−0.013	0.015	0.063
0.01.....	6	7	91	8	0.021	−0.042	0.067
0.10.....	20	7	91	9	−0.064	0.044	0.062
0.18.....	21	6	93	8	−0.031	0.041	0.059
0.31.....	36	5	84	6	−0.112	−0.018	0.052
0.48.....	52	3	67	4	−0.089	0.037	0.039
0.70.....	47	3	63	4	−0.129	0.037	0.044
1.29.....	54	4	67	4	−0.081	−0.009	0.046
3.35.....	47	4	59	4	−0.073	−0.027	0.051

<sup>a</sup> Exposure = 600 s, P.A. =  $160^\circ$ ,  $\sigma_* = 0''.20$ .

<sup>b</sup> Exposure = 900 s, P.A. =  $160^\circ$ ,  $\sigma_* = 0''.22$ .

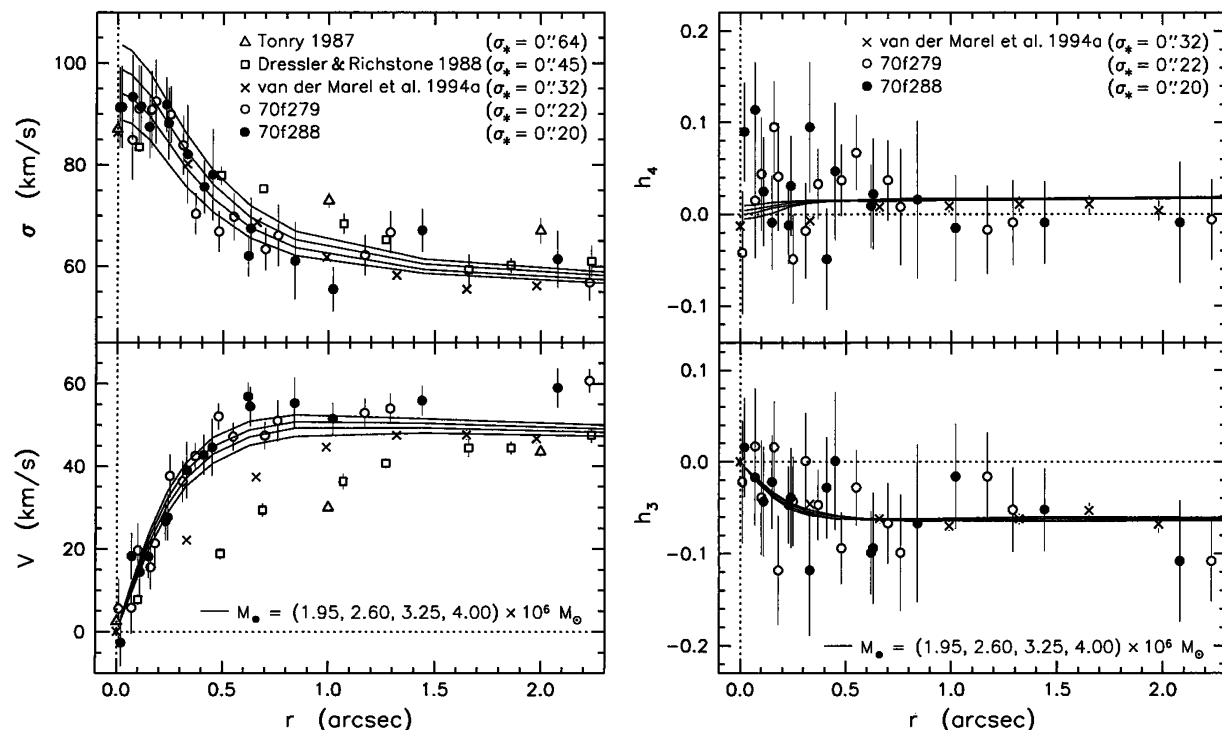


FIG. 2.—Major-axis kinematics of M32 as derived here (70f288 and 70f279) together with data from Tonry (1987), Dressler & Richstone (1988), and van der Marel et al. (1994b). New  $f(E, L_z)$  models were calculated as in Dehnen (1995) and “observed” at resolution  $\sigma_* = 0''.20$ . Assumed BH masses are given in the key.

and parameter coupling. Although we tested and corrected for these effects with the Monte Carlo simulations, we nevertheless were very conservative in our error estimates and included possible bias and error coupling effects. Therefore, the errors in  $h_3$  and  $h_4$  are relatively large, and the FCQ errors in  $V$  and  $\sigma$  are larger than the FQ errors (compare Table 1 here with Fig. 10 in KR95).

### 3. RESULTS

Figure 2 shows our observations of M32 together with new  $f(E, L_z)$  models calculated as in Dehnen (1995) and observed with a resolution of  $\sigma_* = 0''.20$ . Lower resolution data from the literature are shown as well. The central kinematic gradients look steeper as resolution improves. At  $\sigma_* = 0''.20$ , the central rotation curve is much steeper than at lower resolution; it peaks at  $V \approx 56 \pm 3 \text{ km s}^{-1}$  at  $r \approx 0''.70$ . The central dispersion profile is slightly steeper;  $\sigma(0) \approx 92 \pm 5 \text{ km s}^{-1}$ . Figure 10 in KR95 compares the SIS data with the models of van der Marel et al. (1994a) and Dehnen (1995) as seen at the present resolution. The fit is good at large radii. But at  $r \approx 1''.0$ , the rotation velocity and the velocity dispersion are larger in M32 than the old models predict. Therefore the new data imply a larger BH mass than the above authors derived:  $M_\bullet > 2 \times 10^6 M_\odot$ .

The models shown in Figure 2 were calculated as follows (Dehnen 1995): First, for an assumed inclination, the observed surface brightness was deprojected using a Richardson (1972)–Lucy (1974) algorithm to obtain the stellar volume density  $\rho$ . The even part of the distribution function was then recovered, again using a Richardson–Lucy algorithm, assuming a constant stellar mass-to-light ratio  $M/L$  and some  $M_\bullet$ . Finally, we adopted a simple form for the odd part of  $f(E, L_z)$  and

computed the LOSVDs by a Monte Carlo technique that simulated the observational setup. The assumed inclination,  $i = 55^\circ$ , stellar mass-to-light ratio,  $M/L_R = 2.6$ , and odd part of the distribution function were chosen to optimize the agreement with the data at  $r \gtrsim 1''.0$ . The resulting models are closely similar to those of van der Marel et al. (1994a) and Qian et al. (1995). They agree reasonably well with the SIS data provided that  $M_\bullet \approx (3.1 \pm 0.5) \times 10^6 M_\odot$ .

The deprojection does not strongly constrain the central slope of the density profile. In Figure 2, we used  $\rho \propto r^{-1.53}$  (Lauer et al. 1992). However, we also calculated a set of models with  $\rho \propto r^{-1.63}$ . They are closely similar to those in Figure 2 and imply that  $M_\bullet \approx (2.8 \pm 0.5) \times 10^6 M_\odot$ . We adopt  $M_\bullet = (3.0 \pm 0.5) \times 10^6 M_\odot$ .

The general behavior of the rotation and dispersion curves—a gradual rise in  $V(r)$  toward the center until seeing dominates and a very shallow dispersion gradient outside the region dominated by the BH—appears to be characteristic of low-luminosity elliptical galaxies (e.g., also NGC 3377; Kormendy, Evans, & Richstone 1996).

Further indication of a BH may be provided by the LOSVDs. The FCQ program provides a nonparametric measure of the LOSVDs. Figure 3 shows the result at  $r = 0''.02$  together with the spectrum fitted by the standard star spectrum broadened by the LOSVD.

Although the errors for each point inside  $r \approx 0''.2$  are relatively large, several points show a marginally significant positive  $h_4$  contribution to the LOSVD, which means that the LOSVD is more triangular than Gaussian. The observed value,  $h_4 = 0.045 \pm 0.017$  at  $r < 0''.2$ , is near the upper end of the distribution of  $h_4$  values normally seen in elliptical galaxies (Bender, Saglia, & Gerhard 1994). At the resolution of

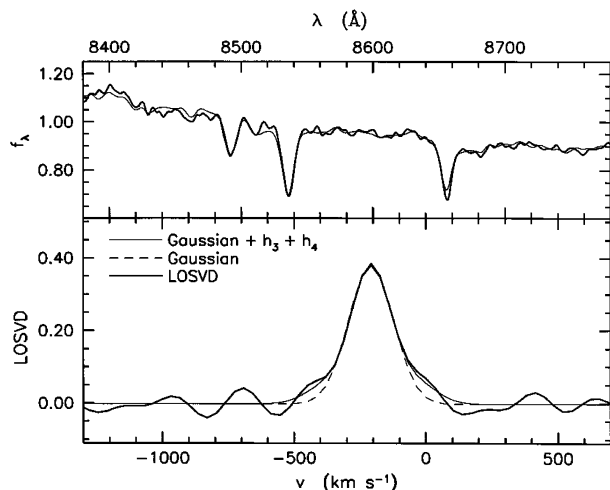


FIG. 3.—*Bottom*: Line-of-sight velocity distribution for the central SIS spectrum of M32. The curves are a Gaussian fit to the core of the LOSVD ( $\sigma = 85 \text{ km s}^{-1}$ ) and one that includes  $h_3$  and  $h_4$ . Note the indication for LOSVD wings. *Top*: Central part of the spectrum (*heavy lines*) and the fit of the broadened, redshifted star spectrum.

published observations of M32, no such wings are seen (van der Marel et al. 1994a, b). We conclude that M32 may contain, very close to the center, stars whose velocities are at least  $200 \text{ km s}^{-1}$  from the local mean. This may or may not by itself be proof of a BH (the existing two-integral models do not predict a positive  $h_4$  for our spatial resolution)—detailed

models are required to interpret the velocities. But large velocities deep in the potential well are most consistent with the BH interpretation. In particular, using  $\eta$ -model machinery from Tremaine et al. (1994; see also Dehnen 1993), we find that, for the observed density distribution, a constant mass-to-light ratio, and an isotropic velocity distribution, the velocity dispersion should decrease toward the center. It should not reach  $\sigma \sim 150\text{--}200 \text{ km s}^{-1}$  at any radius where stars make a significant contribution to the LOSVD.

#### 4. CONCLUSION

M32 has now been observed and modeled by five independent groups. Models without MDOs consistently fail to fit the kinematics. These include maximum entropy models that were instructed to minimize the central  $M/L$ . The available spatial resolution has improved by a factor of 3 since Tonry's (1984, 1987) discovery observations; as resolution and modeling techniques have improved, the MDO case has become more robust. The present SIS data (resolution  $\sigma_* = 0''.20$ ) are well fitted by two-integral models only if  $M_\bullet \simeq (3.0 \pm 0.5) \times 10^6 M_\odot$ .

It is a pleasure to thank Olivier Le Fèvre for his efficient support of the observing run. R. B's work was supported by Sonderforschungsbereich 375 of the German Science Foundation and by the Max-Planck-Gesellschaft. J. K. was supported by NSF grant AST 92-19221. W. D. acknowledges support by PPARC.

#### REFERENCES

- Bender, R. 1990, *A&A*, 229, 441  
 Bender, R., Saglia, R. P., & Gerhard, O. E. 1994, *MNRAS*, 269, 785  
 Dehnen, W. 1993, *MNRAS*, 265, 250  
 ———. 1995, *MNRAS*, 274, 919  
 Dressler, A., & Richstone, D. O. 1988, *ApJ*, 324, 701  
 Kormendy, J. 1988a, *ApJ*, 325, 128  
 ———. 1988b, *ApJ*, 335, 40  
 Kormendy, J., Evans, A. S., & Richstone, D. 1996, in preparation  
 Kormendy, J., & McClure, R. D. 1993, *AJ*, 105, 1793  
 Kormendy, J., & Richstone, D. 1992, *ApJ*, 393, 559  
 ———. 1995, *ARA&A*, 33, 581 (KR95)  
 Lauer, T. R., et al. 1992, *AJ*, 104, 552  
 Lucy, L. B. 1974, *AJ*, 79, 745  
 Moffat, A. F. J. 1969, *A&A*, 3, 455  
 Qian, E. E., de Zeeuw, P. T., van der Marel, R. P., & Hunter, C. 1995, *MNRAS*, 274, 602  
 Richardson, W. H. 1972, *J. Opt. Soc. Am.*, 62, 52  
 Richstone, D. O., & Tremaine, S. 1988, *ApJ*, 327, 82  
 Tonry, J. L. 1984, *ApJ*, 283, L27  
 ———. 1987, *ApJ*, 322, 632  
 Tremaine, S., Richstone, D. O., Byun, Y.-I., Dressler, A., Faber, S. M., Grillmair, C., Kormendy, J., & Lauer, T. R. 1994, *AJ*, 107, 634  
 van der Marel, R. P., Evans, N. W., Rix, H.-W., White, S. D. M., & de Zeeuw, T. 1994a, *MNRAS*, 271, 99  
 van der Marel, R. P., Rix, H.-W., Carter, D., Franx, M., White, S. D. M., & de Zeeuw, T. 1994b, *MNRAS*, 268, 521